Available online at www.sciencedirect.com

ScienceDirect

Geochimica et Cosmochimica Acta 247 (2019) 27–39

Geochimica et Cosmochimica Acta

www.elsevier.com/locate/gca

Annually-resolved coral skeletal $\delta^{138/134}$Ba records: A new proxy for oceanic Ba cycling

Yi Liu [a,b,*], Xiaohua Li [a], Zhen Zeng [a], Hui-Min Yu [a,*], Fang Huang [a], Thomas Felis [c], Chuan-Chou Shen [d,e]

[a] *CAS Key Laboratory of Crust-Mantle Materials and Environments, School of Earth and Space Sciences, University of Science and Technology of China, Hefei 230026, China*

[b] *Institute of Surface-Earth System Science, Tianjin University, Tianjin 300350, China*

[c] *MARUM-Center for Marine Environmental Sciences, University of Bremen, 28359 Bremen, Germany*

[d] *High-Precision Mass Spectrometry and Environment Change Laboratory (HISPEC), Department of Geosciences, National Taiwan University, Taipei 10617, Taiwan*

[e] *Research Center for Future Earth, National Taiwan University, Taipei 10617, Taiwan*

Received 3 May 2018; accepted in revised form 15 December 2018; Available online 21 December 2018

Abstract

Barium/calcium ratios in the skeletons of scleractinian shallow-water corals have been used as proxies for coastal and oceanic processes such as river discharge, oceanic upwelling and surface ocean productivity. However, the variations in Ba/Ca ratios in aragonitic coral skeletons remain difficult to interpret as an environmental proxy. This difficulty is mainly due to the influence of internal (biomineralization) and multiple external (environmental) processes on Ba incorporation into coral skeletons, and these processes are hard to constrain with Ba/Ca alone. Here we present the first annually-resolved records of the Ba isotopic compositions ($\delta^{138/134}$Ba) in shallow-water corals (*Porites*) collected alive in the field, supplemented by the analysis of Ba/Ca ratios. Seven coral cores were recovered at different oceanic settings in the South China Sea, extending from the northern inner shelf to the central and southern deep basin. The annual $\delta^{138/134}$Ba records of six corals fell within a narrow range from 0.24 ± 0.03‰ to 0.38 ± 0.03‰ (2SD), with a mean value of 0.33 ± 0.08‰ (2SD, $N = 21$). One single inner-shelf coral revealed low $\delta^{138/134}$Ba values ($0.10 \sim 0.11 \pm 0.03$‰), which might reflect the influence of terrestrial water/sediment. In contrast, the coral Ba/Ca ratios showed a wide range of intercolony differences, from 2 to 14 μmol/mol. This variation is too large to be ascribed to the changes in the Ba concentrations of seawater or other environmental parameters. Rayleigh fractionation between corals and seawater during biomineralization was proposed to explain the anomalous variations in the Ba/Ca ratios observed in coral skeletons. However, this result is incompatible with the relatively constant Ba isotopic compositions in coral. Instead, we suggest that the probable precipitation of witherite ($BaCO_3$) within the domains of aragonite under oversaturated calcifying fluid could explain the large variability in the coral Ba/Ca ratios. The coral $\delta^{138/134}$Ba records from diverse oceanic settings were largely unaffected by biomineralization processes and temperature and displayed a relatively constant negative offset from typical surface seawaters. Our results suggest that Ba isotopes in *Porites* could be a proxy for reconstructing the $\delta^{138/134}$Ba of seawater and hence provide new insights into Ba cycling in the upper oceans in the past.

Keywords: Barium isotopes; Ba/Ca; *Porites* corals; Biomineralization; South China Sea; Oceanic barium cycle

* Corresponding authors at: CAS Key Laboratory of Crust-Mantle Materials and Environments, School of Earth and Space Sciences, University of Science and Technology of China, Hefei 230026, China (Y. Liu).

E-mail addresses: gee@ustc.edu.cn (Y. Liu), huy16@ustc.edu.cn (H.-M. Yu).

https://doi.org/10.1016/j.gca.2018.12.022

1. INTRODUCTION

Barium (Ba) cycling in the oceans is controlled by riverine inputs, nutrient cycling, marine productivity and ocean circulation (Bishop, 1988; Paytan and Kastner, 1996; Dehairs et al., 1997; Jacquet et al., 2005). Near coasts, Ba in surface seawater is mainly supplied from freshwater discharge/sediment loads and shows highly variable concentrations (Shaw et al., 1998; Weldeab et al., 2007). In the water columns of open oceans, dissolved Ba shows a nutrient-type distribution, which is driven by precipitation of barite ($BaSO_4$) associated with the decay of organic matter (Bishop, 1988). These unique features have led to the development of a number of Ba-based proxies to study modern and paleo-oceans (Paytan and Griffith, 2007; Weldeab et al., 2007).

Recently, with the advancement of high precision methods for nontraditional isotope analyses, Ba isotopes ($\delta^{138}/^{134}Ba$) have been used to study different environmental processes (Miyazaki et al., 2014; Nan et al., 2015; Bullen and Chadwick, 2016; Bridgestock et al., 2018). Significant Ba isotopic fractionations between solutions and minerals have been revealed in both field and artificial precipitation experiments, and the light isotopes were found to be enriched in the mineral phase (von Allmen et al., 2010; Mavromatis et al., 2016; Böttcher et al., 2018, in press). In particular, several studies have introduced Ba isotopes in seawater as a new tracer for investigating Ba cycling in the oceans (Horner et al., 2015; Cao et al., 2016; Bates et al., 2017; Hsieh and Henderson, 2017; Bridgestock et al., 2018). These studies showed considerable variations in $\delta^{138/134}Ba$ (0.25–0.60‰) in global seawaters with different depths (Hsieh and Henderson, 2017). The $\delta^{138}/^{134}Ba$ values were found to decrease with water depth, and this decrease was accompanied by an increase in dissolved Ba concentrations ([Ba]), which is closely related to barite precipitation in the upper ocean and remineralization in the deep ocean (Horner et al., 2015; Cao et al., 2016; Bridgestock et al., 2018). Moreover, riverine inputs that carry light Ba isotopes can also significantly affect the Ba isotopes of nearby surface seawaters (Cao et al., 2016; Hsieh and Henderson, 2017).

Scleractinian corals with aragonite skeletons are abundant in the global surface ocean throughout the tropics to subtropics. The various trace elements and stable isotopic compositions of coral skeletons have provided continuous centennial-scale records of the past physical and chemical properties of the ocean at high (annual-seasonal) resolution (Felis and Pätzold, 2003; Saha et al., 2016). In recent decades, Ba/Ca ratios in shallow-water corals have been widely used to reconstruct changes in the Ba concentrations of seawater driven by riverine/groundwater inputs, upwelling, and productivity (Lea et al., 1989; McCulloch et al., 2003; Montaggioni et al., 2006; Alibert and Kinsley, 2008; Moyer et al., 2012; LaVigne et al., 2016; Saha et al., 2016). However, the incorporation of seawater Ba signals into corals can be disturbed by the 'vital effects' that accompany coral growth and/or multiple environmental factors (e.g., temperature) (Gaetani and Cohen, 2006; Gonneea et al., 2017). This disturbance is exemplified by the consistently unexplained high amplitude and high frequency of variations in the Ba/Ca ratios recorded in coral skeletons (Tudhope et al., 1996; Sinclair, 2005; Pretet et al., 2016). In addition, Ba/Ca ratios alone cannot provide information about the local Ba inputs or related changes throughout the oceanic Ba cycle (Hemsing et al., 2018). Barium isotopes in corals may complement the existing Ba proxies and have the potential to be a new proxy for historical Ba cycling in the oceans. However, the Ba isotopic systematics of shallow-water coral remain poorly constrained because of the analytical difficulties in purifying Ba from corals with low Ba concentrations and extremely high Ca/Ba ratios. Only one study reported $\delta^{138/134}Ba$ data from aragonite shallow-water corals, which showed light Ba isotopic compositions compared to ambient seawater (Pretet et al., 2016). As noted by the authors, the large analytical uncertainty ($2SD > \pm 0.1‰$) and sample resolution (bulk) did not allow for a detailed study on the Ba isotopic fractionation in those corals (Pretet et al., 2016). A recent study provided important insights regarding the paleoceanographic potential of Ba isotopes in the aragonite skeletons of cold/deep water corals (Hemsing et al., 2018).

In this study, we precisely determined the Ba isotopic compositions of modern *Porites* corals with an annual resolution using the multicollector inductively coupled plasma mass spectrometry (MC-ICP-MS) technique. The instrumental mass bias of Ba isotopes was corrected using the double spike method. *Porites* is the most widely used species for the study of coral-based paleoceanographic reconstruction in the Indo-Pacific Ocean. Seven *Porites* colonies were collected from contrasting physical-biogeochemical sites of the South China Sea (SCS), extending from the shallow inner shelf to the deep basin. The main aim of this study is to evaluate (i) the environmental factors controlling the incorporation of Ba into aragonite shallow-water corals, (ii) the biological influences on Ba isotopic fractionation, and (iii) the potential of using Ba isotopes as paleoceanographic proxies.

2. MATERIALS AND METHODS

2.1. Sample sites

The SCS is located at 4–25 °N and 109–121 °E and is one of the largest marginal seas in the world. The SCS has both deep basins and extensive shelf systems along the northern and southern boundaries associated with large riverine and sediment inputs mainly from the Pearl, Red, and Mekong Rivers. The SCS seawater is also exchanged with the western Pacific seawater through the Luzon Strait, which has a depth of 2000 m. Seven cores from living *Porites* colonies were collected from three physical-biogeochemical domains across the SCS: the Luzon Strait domain (Xiaoliuqiu-XLQ and Nanwan-NW), the northern coast domain (Longwan-LW, Xiaodonghai-XDH and Weizhou Island-WZI), and the open ocean domain (Yongxing Island-YXI and Yongshu Reef-YSR) (Fig. 1; Table 1). The Luzon Strait domain is located along the southern coast of Taiwan and is strongly influenced by western Pacific waters. The northern coast domain is influ-

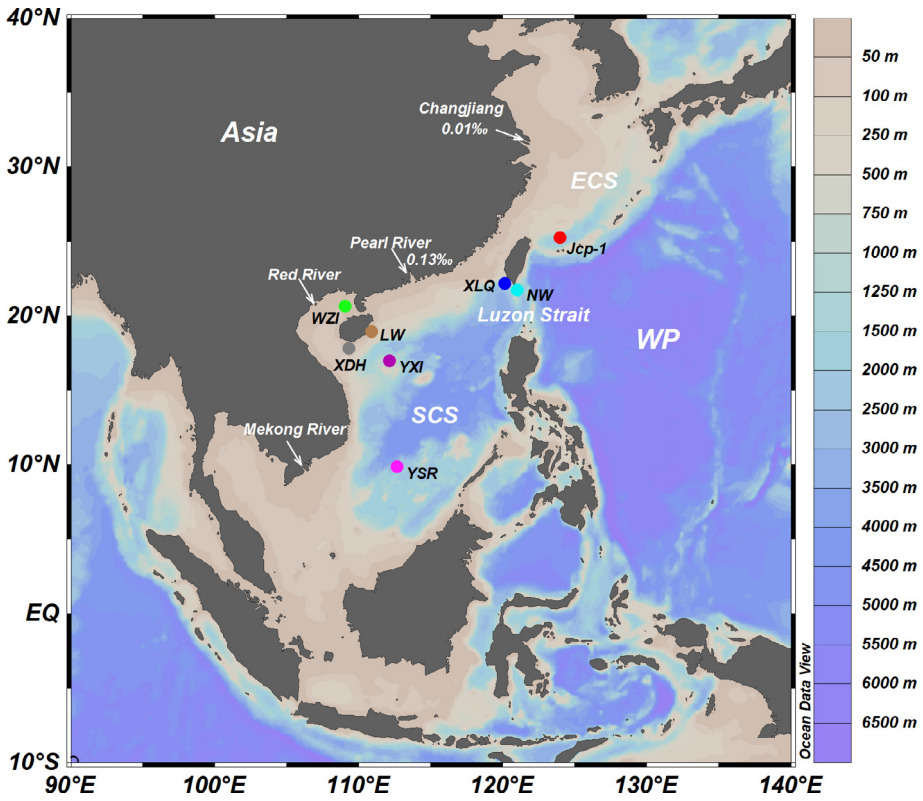

Fig. 1. Bathymetric map of the South China Sea (SCS) and the East China Sea (ECS) generated by Ocean Data View (Schlitzer, 2018). The Changjiang River, Pearl River, Red River and Mekong River are shown, which feed the ECS and SCS. Circles denote locations of seven *Porites* coral cores, Xiaoliuqiu (XLQ), Nanwan (NW), Weizhou Island (WZI), Longwan (LW), Xiaodonghai (XDH), Yongxing Island (YXI) and Yongshu Reef (YSR). The international coral standard JCp-1 was from Ishigaki Island near the ECS (Okai et al., 2002). The $\delta^{138/134}$Ba values of the Changjiang and the Pearl Rivers (Cao et al., 2016) are also shown. WP: Western Pacific.

enced by high terrestrial water/sediment inputs from the East Asian continent. The open ocean domain is located in the central and southern deep basin of the SCS, which represents a tropical oligotrophic environment with low productivity.

Sea surface temperature (SST) data at 1° spatial resolution for the seven sample sites were obtained from Reynolds et al. (2002) (http://iridl.ldeo.columbia.edu/SOURCES/.NOAA/.NCEP/.EMC/.CMB/.GLOBAL/.Reyn_SmithOIv2/.monthly/.sst/). Rainfall data at 0.5° spatial resolution were obtained from Becker et al. (2011) (https://www.esrl.noaa.gov/psd/data/gridded/data.gpcc.html). Chl-a concentrations at 0.4° spatial resolution were obtained from the AQUA/MODIS satellite dataset (National Aeronautics and Space Administration (NASA), http://oceancolor.gsfc.nasa.gov/). The annual mean SST range for these sites is ~25–29 °C. Rainfall ranges varied from 140 to 230 cm/a, and the Chl-a concentrations varied from 0.15 to 2.3 mg/m^3 (Table 1).

2.2. Chemical purification and isotopic analyses

Five-mm-thick slabs from each *Porites* coral core were cut, washed with ultrapure water, and dried for X-ray image processing. All slabs exhibit clear and regular annual density banding patterns (Supplementary Fig. S1). Powder X-ray diffraction analysis revealed the absence of calcite (<1%) in coral samples, and scanning electron microscopy results showed an absence of secondary aragonite cements. Coral slabs were kept in 10% H_2O_2 for 24 h to decompose organic matter and then washed with ultrapure water by ultrasonic cleaning three times (20 minutes each). Annual subsamples were milled along the axis of maximum growth in these cleaned slabs. Specifically, subsamples from 1987 to 1991 were taken from XLQ, NW, WZI, LW, XDH, YXI and YSR. Additional subsamples from 1984, 1986, 1995–1998 and 2002 were taken from NW and 1996–2000 from XDH. After grounding into a homogeneous powder using precleaned agate, ~150 mg powder of each subsample was digested for Ba/Ca and Ba isotope measurements. A standardized coral powder, JCp-1 (Geological Survey of Japan), which was a *Porites* colony from Ishigaki Island in the East China Sea (ECS), was also analyzed in this study (Fig. 1; Okai et al., 2002; Hathorne et al., 2013).

After being completely digested using concentrated HNO_3, HF, and HCl, 48 subsamples in total were dissolved in 3% HNO_3 and analyzed for Ba/Ca ratios on an Elan DRCI Quadrupole ICP-MS at the CAS Key Laboratory of Crust-Mantle Materials and Environments, University of Science and Technology of China (USTC), Hefei. An in-house standard was measured once in every five sample measurements to correct for instrumental drift. The coral standard JCp-1 was analyzed twice in each sequence. The external precision was ±3% (RSD).

Table 1
The information of sample sites and *Porites* coral samples.

Sample site	Sampling date	Latitude/Longitude N/E	Domain	Depth (m)	Growth rate (cm/a)	SST (°C)	Rainfall (cm/a)	Chl-a (mg/m^3)
Xiaoliuqiu (XLQ)	2003.8	22°19′/120°23′	Luzon Strait, southwest coast of Taiwan	5	1.5	26.3	168.3	0.35
Nanwan (NW)	2006.5	21°56′/120°44′	Luzon Strait, southern coast of Taiwan	5	1.9	26.9	223.1	0.17
Weizhou Island (WZI)	2009.9	21°01′/ 109°04′	Northern coast, inner shelf	7	0.7	25.4	158.4	2.32
Longwan (LW)	1998.8	19°20′/110°39′	Northern coast, east of Hainan Island	5	0.9	26.1	170.1	0.66
Xiaodonghai (XDH)	2002.4	18°10′/109°30′	Northern coast, south of Hainan Island	5	2.5	26.5	139.8	0.43
Yongxing Island (YXI)	1993.6	16°49′/112°20′	Open ocean, central deep basin	5	1.0	27.5	151.3	0.17
Yongshu Reef (YSR)	1993.6	9°38′/112°53′	Open ocean, southern deep basin	5	1.1	28.6	232.4	0.15

For Ba isotope analyses, Ba purification was performed in an ISO-class 6 clean room at the USTC following the methods in Zeng et al. (2019). All reagents that were used were diluted from double-distilled acids with 18.2 MΩ·cm ultrapure water. Subsamples containing 500 ng Ba were digested in 2 mol L^{-1} HCl, and a double spike pair of ^{135}Ba-^{136}Ba (ISOFLEX) was added during sample digestion to correct for mass fractionation during chemical purification and instrumental analysis. After dryness, the spiked subsample was dissolved in 2 mL 3 mol L^{-1} HCl for chromatographic separation. All information on the ion exchange chromatography procedures was described in detail by Zeng et al. (2019). We only briefly describe the different steps in this study. The first two ion exchange columns with AG50W-X12 resin (200–400 mesh, Bio-Rad, USA) were used to elute most matrix elements with 3 mol L^{-1} HCl, and then Ba was collected with 4 mol L^{-1} HNO_3. After these two columns, the Ca/Ba ratios in the sample solutions were less than 10, which is too low to affect the Ba isotope measurements. The third column with 0.5 mL AG50W-X12 resin was used to further separate Ba from Ce, which are isobaric isotopes of ^{136}Ba and ^{138}Ba. Subsamples in 1 mL 2 mol L^{-1} HNO_3 were loaded into the third column and washed with 5 mL 2 mol L^{-1} HNO_3. Barium was collected with 18 mL 2 mol L^{-1} HNO_3. After dryness, the sample was dissolved in 2% HNO_3 to 100 ng g^{-1} for instrumental analysis. The whole procedure blank was only 0.2 ng, which would not cause a significant bias in the Ba isotopic compositions of coral samples.

Barium isotopic compositions were analyzed on MC-ICP-MS at the USTC (Neptune Plus from Thermo-Fisher Scientific of Bremen, Germany). The cup configuration was set as follows: ^{131}Xe, ^{134}Ba, ^{135}Ba, ^{136}Ba, ^{137}Ba and ^{140}Ce were collected on Faraday cups of L4, L2, L1, C-cup, H1 and H3 in static mode. All instrumental parameters followed those reported in Zeng et al. (2019).

The Ba isotopic compositions are expressed as $\delta^{138/134}Ba_{SRM3104a} = [(^{138/134}Ba_{sample})/(^{138/134}Ba_{SRM3104a}) - 1] \times 1000$, where SRM3104a is a $Ba(NO_3)_2$ standard solution provided by the National Institute of Standards and Technology (NIST). The results for the $^{138/134}$Ba isotope pair were obtained considering mass-dependent isotope fractionation by multiplying the measured mass $\delta^{137/134}Ba_{SRM3104a}$ results by a factor of 1.33 (Pretet et al., 2016).

Uncertainties of Ba isotopic data are calculated at 2 × SD (standard deviation) unless otherwise noted. Long-term measurements of $\delta^{138/134}$Ba data (0.30 ± 0.03‰, N = 11, Supplementary Fig. S2) for the JCp-1 coral standard match the previous values of 0.29 ± 0.03‰ by Horner et al. (2015), 0.26 ± 0.11‰ by Pretet et al. (2016) and 0.25 ± 0.03‰ by Hemsing et al. (2018) (the calculation details are provided in the supplementary material).

3. RESULTS

The Ba/Ca ratios and $\delta^{138/134}$Ba data are listed in Table 2. The coral Ba/Ca ratios varied spatially and temporally from 2.11 to 13.79 μmol/mol, which is within the

Table 2
Annual Ba/Ca ratios and Ba isotopic compositions in *Porites* corals.

Sample	Year	Ba/Ca (μmol/mol)	$\delta^{137/134}$Ba (‰)	2SD[a]	$\delta^{138/134}$Ba (‰)[b]	n[c]
XLQ	1987	2.12				
	1988	2.11				
	1989	2.27	0.25	0.02	0.33	2
	1990	2.16				
	1991	2.21				
NW	1983	2.33	0.27	0.00	0.36	2
	1986	3.33	0.29	0.01	0.38	2
	1987	3.26	0.27	0.01	0.36	2
	1988	3.56				
	1989	3.23				
	1990	2.87	0.26	0.01	0.34	2
	1991	3.27	0.26	0.03	0.35	4
	1995	3.05	0.26	0.03	0.35	2
	1996	2.44	0.27	0.04	0.36	2
	1997	2.56	0.28	0.02	0.38	7
	1998	2.90	0.26	0.00	0.34	2
	2002	2.91	0.28	0.01	0.37	5
WZI	1987	8.40	0.08	0.04	0.10	2
	1988	9.19				
	1989	9.76	0.08	0.03	0.11	3
	1990	9.17				
	1991	9.27				
LW	1987	11.74	0.20	0.01	0.26	4
	1988	8.92	0.23	0.04	0.30	2
	1989	7.78				
	1990	8.27				
	1991	9.00	0.18	0.04	0.24	2
XDH	1987	3.72				
	1988	3.70				
	1989	3.56				
	1990	3.75	0.25	0.04	0.33	4
	1991	4.41				
	1996	4.20	0.23	0.01	0.30	2
	1997	5.02				
	1998	6.45				
	1999	7.48				
	2000	8.34	0.18	0.04	0.24	2
YXI	1987	3.75	0.24	0.00	0.32	2
	1988	3.31				
	1989	2.74				
	1990	2.53				
	1991	2.48				
YSR	1987	12.96	0.23	0.02	0.33	2
	1988	12.89				
	1989	11.37	0.26	0.01	0.34	2
	1990	13.57				
	1991	13.87	0.27	0.04	0.36	4

[a] SD is the standard deviation of the population of repeat measurements of a single sample solution. The external reproducibility of the Ba isotope measurements is ±0.03‰ (Fig. S1).
[b] $\delta^{138/134}$Ba were recalculated from measured $\delta^{137/134}$Ba values as described in the text.
[c] n is the times of repeated measurements of the same solution.

reported range in corals (Gonneea et al., 2017). The average Ba/Ca ratios in corals from XLQ and NW along the southern coast of Taiwan (Luzon Strait domain) are 2.16 and 3.47 μmol/mol, respectively. The inner-shelf coral from WZI and the two near-shelf corals from LW and XDH (northern coast domain) have high average Ba/Ca ratios of 9.30, 8.92 and 6.29 μmol/mol, respectively. The YXI coral and YSR coral from the deep basin (open ocean domain) show very different Ba/Ca ratios. The average Ba/Ca ratio of YXI coral is only 2.93 μmol/mol, but the

average Ba/Ca ratio of YSR coral is as high as 12.97 μmol/mol. Moreover, the annual Ba/Ca ratios of the XDH coral show an increasing trend from 1987-2000 (Fig. 2A).

In contrast to the large variations in the Ba/Ca ratios, the Ba isotopic compositions of the studied corals (excluding the inner-shelf coral from WZI) are within a narrow range from $0.24 \pm 0.03‰$ to $0.38 \pm 0.03‰$, with a mean value of $0.33 \pm 0.08‰$ (Fig. 2B). There is no correlation between $\delta^{138/134}$Ba values and Ba/Ca ratios. In particular, the annual $\delta^{138}/^{134}$Ba values in NW do not exhibit any

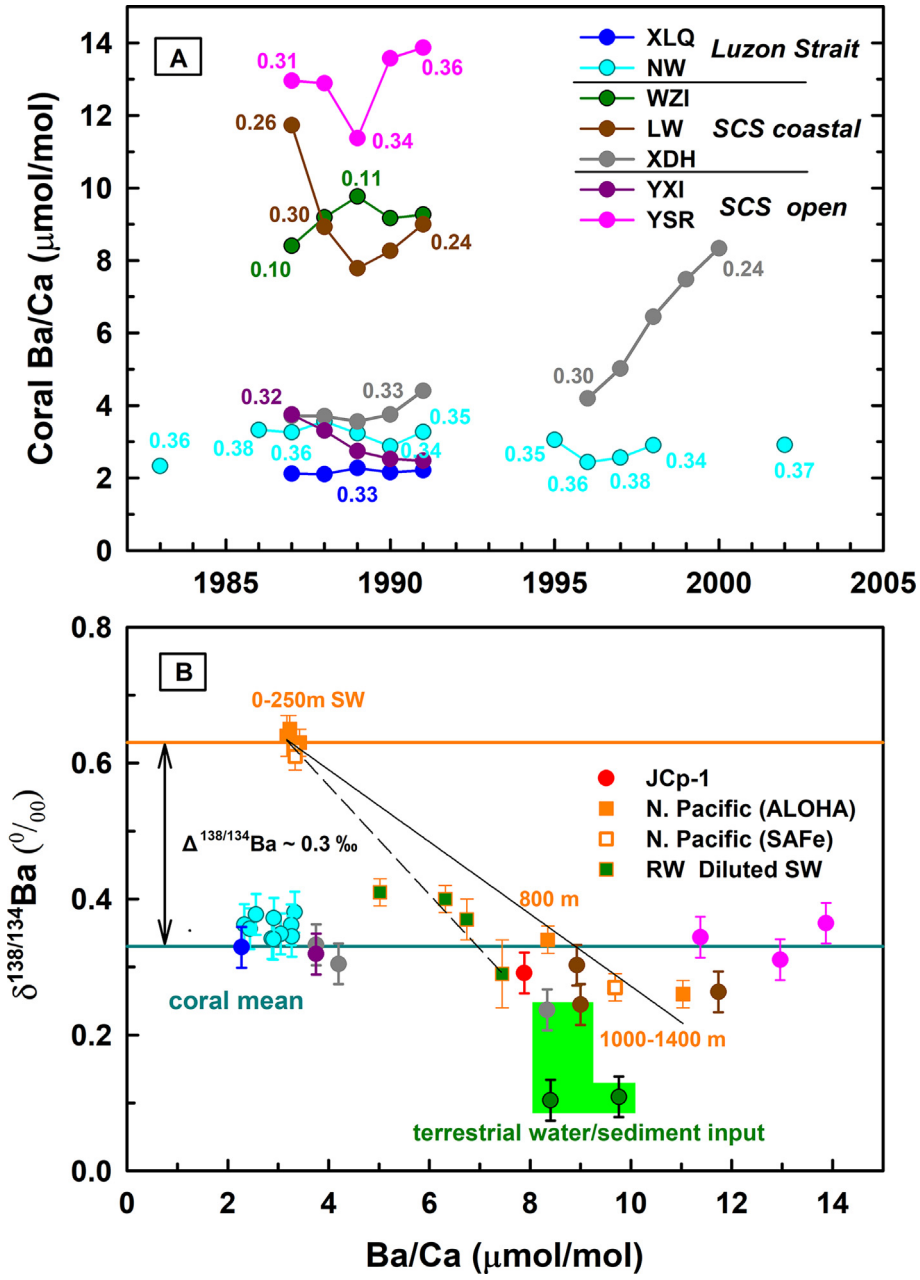

Fig. 2. (A) The annual variations in Ba/Ca ratios in seven *Porites* corals from the South China Sea (SCS) with corresponding $\delta^{138/134}$Ba values indicated (unit: ‰). (B) The $\delta^{138/134}$Ba values against the Ba/Ca ratios of the *Porites* corals (circles). Error bars represent 2 standard deviations (2SD) of the external long-term reproducibility of $\delta^{138/134}$Ba measurements. Excluding the WZI coral (green circles), the mean $\delta^{138/134}$Ba value in our corals (solid dark cyan line, $0.33 \pm 0.08‰$, 2SD) is within the uncertainty of the coral reference material JCp-1 ($0.30 \pm 0.03‰$, red circle). Orange squares represent seawater (SW) (0–1400 m) of the North Pacific [ALOHA and SAFe stations, Hsieh and Henderson (2017)]. Green squares represent river water (RW)-diluted SW (Hsieh and Henderson, 2017). The solid black line indicates the vertical mixing between the surface SW and the deep SW. The dashed black line indicates the horizontal mixing between the surface SW and the RW-diluted SW. The *Porites* $\delta^{138/134}$Ba values from the SCS display an offset of $\Delta^{138/134}$Ba $\sim -0.3‰$ from the surface SW. The $\delta^{138/134}$Ba of JCp-1 display a similar offset of $\Delta^{138/134}$Ba $\sim -0.3‰$ from the surface SW. Some of the scatter in the coral data (in green shading) is suspected to be affected by terrestrial water/sediment inputs. (For interpretation of the references to color in this figure legend, the reader is referred to the web version of this article.)

significant variations throughout the study period (1983–2002). The mean $\delta^{138}/^{134}$Ba value of SCS corals is identical to the JCp-1 coral standard (0.30 ± 0.03‰). The WZI corals have the lowest $\delta^{138/134}$Ba values of 0.10 ± 0.03‰ and 0.11 ± 0.03‰.

4. DISCUSSION

4.1. Barium isotopes of *Porites* corals

Compared to the $\delta^{138/134}$Ba variations from 0.52 to 0.62‰ that are typical in surface seawaters throughout the world (Hsieh and Henderson, 2017), the *Porites* corals across the diverse sites of the SCS have low $\delta^{138}/^{134}$Ba values. The preferential incorporation of the light Ba isotopes in the carbonate is a common feature for other earth alkaline and alkali isotope systems, such as Ca, Mg, Sr, and Li (e.g., Wombacher, et al., 2011; Raddatz et al., 2013; Inoue et al., 2015; Fruchter et al., 2016). The fractionation has been interpreted as a result of a kinetic effect combined with biological effects (Wombacher, et al., 2011; Inoue et al., 2015).

4.1.1. Effects of different parameters on Ba isotopes of Porites corals

To explore the potential controls on Ba isotopic compositions in corals, we compared the coral $\delta^{138/134}$Ba to coral growth rates and regional and local environmental parameters (Fig. 3). In this study, despite a wide range of growth rates from 0.7 to 2.5 cm/a, $\delta^{138/134}$Ba seems to be independent of coral growth rates. One exception was the WZI coral that had the lowest growth rates and the lowest $\delta^{138/134}$Ba, which might indicate an impact from the low growth rate. However, based on the kinetic incorporation model, a sharp decrease in the growth rate will reduce the isotope fractionation of Ba towards that characteristic for equilibrium isotope partitioning. In this case, the mineral phase is supposed to be isotopically heavier rather than the opposite direction observed in this study (Wombacher, et al., 2011; Hofmann et al., 2012; Mavromatis et al., 2016). Similarly, Inoue et al. (2015) and Fruchter et al. (2016) did not observe a clear growth-rate dependence on $\delta^{44/40}$Ca and $\delta^{88/86}$Sr of corals. Abiotic precipitation [witherite ($BaCO_3$)] experiments also revealed different correlations between precipitation rates and Ba isotope fractionation. Böttcher et al. (2018, in press) obtained a positive correlation between precipitation rate and Ba isotope fractionation, while the opposite relationship was observed by von Allmen et al. (2010) and Mavromatis et al. (2016). A large magnitude of Ba isotope fractionation upon $BaCO_3$ formation can be found under both slow and fast precipitation conditions.

The sampling sites in our study cover a SST range from ~25 °C to 29 °C (Table 1). There is no correlation between $\delta^{138/134}$Ba and SST (Fig. 3D). Although the WZI coral has the lowest $\delta^{138/134}$Ba at the lowest growth temperature, all of the other corals have similar Ba isotopes at different SSTs. Hemsing et al. (2018) also did not find temperature dependence of $\delta^{138/134}$Ba in cold water/deep water corals at a much lower temperature (<3 °C). Our results are also consistent with the results of abiotic precipitation experiments in which Ba isotope fractionation was consistent between 4 and 80 °C (von Allmen et al., 2010; Böttcher et al., 2018, in press). The relationship between the $\delta^{138/134}$Ba values and rainfall is also negligible (Fig. 3F).

Some of the scatter in our coral $\delta^{138/134}$Ba data is most likely caused by local changes in the seawater Ba isotopic composition. For example, the WZI coral with the lowest $\delta^{138/134}$Ba is located at the northern inner shelf, which received a much higher terrigenous sediment flux than all other sites. A large amount of Ba could be desorbed from riverine sediments, which occurs upon seawater mixing (McCulloch et al., 2003). The southern part of Hainan Island, where the XDH coral is located, is one of the most popular tourist destinations in China with beaches and resorts. The low coral $\delta^{138/134}$Ba value (0.24‰) at XDH in 2000 (Fig. 2A) could be the result of the construction of infrastructure along the coastline in recent years. Interestingly, a negative correlation between the Ba isotopes and Chl-a concentrations ($R = -0.94$, $p < 0.001$) was observed in this study (Fig. 3H). WZI is located along the inner shelf and experiences the highest Chl-a concentration while it has the lowest $\delta^{138/134}$Ba values. In contrast, YSR and YXI are open ocean sites, and NW is located at the south coast of Taiwan and faces the open western Pacific; these sites experience the lowest Chl-a concentrations and have the highest $\delta^{138/134}$Ba values. It is a robust feature that a significant correlation ($R = -0.78$, $p < 0.001$) still exists when WZI is not considered (gray regression line, Fig. 3H). This negative correlation between surface water Chl-a and coral $\delta^{138/134}$Ba could be produced by the terrestrial influence from both parameters in marginal seas (Fig. 3H), such as the SCS. Terrestrial water/sediment inputs not only bring nutrients that support phytoplankton blooms but also decrease $\delta^{138/134}$Ba values, which has been observed in the Pearl River area ($\delta^{138/134}$Ba = 0.08‰) by Cao et al. (2016).

4.1.2. Estimation of $\Delta^{138/134}$Ba between Porites corals and seawater

Our results show that the $\delta^{138/134}$Ba in *Porites* corals from diverse marine settings of the SCS is relatively constant and largely independent of other environmental influences. This result suggests that *Porites* corals act as a potential archive to record the Ba isotopic compositions of the surface ocean and could provide new information on freshwater discharge/sediment loads and marine productivity in the past. Before coral skeletons can be used as archives, we need to determine the fractionation factor between coral and ambient seawater. Although the $\delta^{138/134}$Ba seawater data are currently not available for the study sites, the global upper ocean shows a relatively homogeneous Ba isotopic composition (with variability <0.1‰) in the surface waters, except for the seawater in areas near river inputs or with strong upwelling, which have distinct Ba isotope signatures (Hsieh and Henderson, 2017; Bridgestock et al., 2018). In this study, the $\Delta^{138/134}Ba_{coral\text{-}sw}$ was estimated from shallow-water corals of the SCS and the upper seawater of the North Pacific (ALOHA and SAFe stations, <250 m water depth) (Hsieh and

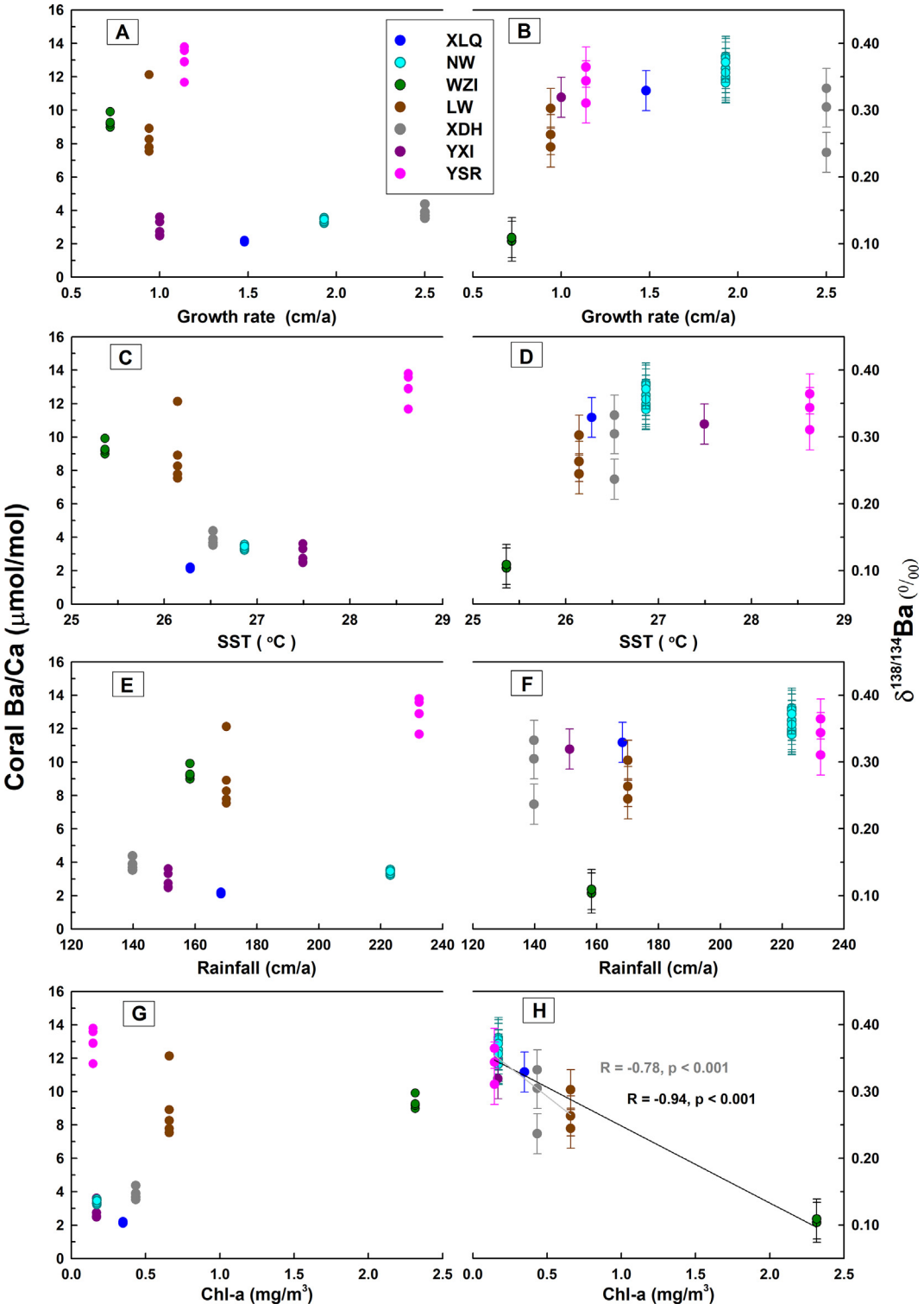

Fig. 3. Correlations between Ba/Ca ratios and $\delta^{138/134}$Ba values of seven *Porites* corals from the South China Sea with coral growth rates and environmental parameters.

Henderson, 2017), which provides an average value ~−0.3‰ for $\Delta^{138/134}Ba_{coral\text{-}SW}$ (Fig. 2B). The magnitude and sign of the calculated $\Delta^{138/134}Ba_{coral\text{-}SW}$ (~−0.3‰) are in good agreement with the value (−0.21‰) identified for cold water/deep water corals in the Atlantic (Hemsing et al., 2018). In addition, our estimated $\Delta^{138/134}Ba_{coral\text{-}SW}$ is also within the range of that measured by previous reports for the precipitation of witherite ($BaCO_3$: −0.12 ~ −0.53‰) or double carbonate norsethite [$BaMn(CO_3)_2$: −0.15‰] (von Allmen et al., 2010; Böttcher et al.,

2018, in press). Moreover, the coral standard (JCp-1 *Porites*) from the western Pacific has the same offset of $\Delta^{138/134}Ba = \sim -0.3‰$ from the surface seawater of the North Pacific. Surely, $\delta^{138/134}Ba$ measurements of in situ seawaters in the near future would provide a better estimate of the isotope fractionation factor between shallow-water corals and ambient seawater.

4.2. Ba/Ca ratios of *Porites* corals

In contrast to the consistent $\delta^{138/134}Ba$ of corals, the Ba/Ca ratios in corals across the SCS represent considerable spatial variations (Fig. 2A). Previous studies found that temperature played a role in the incorporation of trace elements in coral skeletons (Gaetani and Cohen, 2006; Saha et al., 2016). Experiments on abiotic aragonite precipitation show that the distribution coefficient between aragonite and fluid ($K_D^{Ba/Ca}$) is inversely related to temperature ($\ln K_D^{Ba/Ca} = 2913/T - 9.0$, Gaetani and Cohen, 2006). The aragonite that precipitates at a high temperature has a lower Ba/Ca ratio than the aragonite that precipitates at a low temperature. However, the observed amplitude of Ba/Ca is approximately 6 times higher the amplitude predicted from the known SST range at the sample sites and the Ba/Ca temperature dependence (Gaetani and Cohen, 2006; Gonneea et al., 2017). This result suggests that temperature is not the main cause of the variation in the Ba/Ca ratio in the studied corals. Similarly, no effects of other ambient environmental parameters were found (Fig. 3E and G). If we assumed Ca concentrations of 9.52 mmol/g in *Porites* coral and 10.28 mmol/kg in seawater (Bruland and Lohan, 2003) and used $K_D^{Ba/Ca}$ values of 2.11 at 25 °C and 1.90 at 29 °C (Gaetani and Cohen, 2006), the calculated [Ba] values of the sea surface water at the coral sites were between 10 and 75 nmol/kg. The range of calculated [Ba] is much higher than the concentrations currently observed in nature (Hsieh and Henderson, 2017). Combined with $\delta^{138/134}Ba$, the varied Ba/Ca ratios cannot be explained by the mixing of three major water masses (i.e., surface, deep and river-diluted seawater) (Fig. 2B). The deep and river-diluted seawater are characterized by higher Ba/Ca ratios and distinctly lower isotopic compositions than surface seawater. However, all corals in this study have similar Ba isotopes.

In summary, the large amplitude of the Ba/Ca ratios in corals cannot be reconciled by a unique $K_D^{Ba/Ca}$ value or correlated to external parameters. The above results point to strong physiological controls on the incorporation of Ba in *Porites* corals, which we will discuss below.

4.3. Effects of biomineralization on the incorporation of Ba in *Porites* coral

In addition to seawater compositions and environmental factors, the incorporation of elements into corals could also be affected by biological factors known collectively as "vital effects" (Gaetani and Cohen, 2006; Rollion-Bard et al., 2010; Wombacher, et al., 2011; Inoue et al., 2015). The new information from paired Ba isotopic compositions and Ba/Ca ratios allows us to explore the effects of biomineralization on the process of Ba incorporation into coral skeletons.

The main hypothesis to explain the vital effects in corals is that the elemental ratios in the coral skeleton were controlled by the Rayleigh fractionation process, in which corals precipitate their skeletons from an isolated or semi-isolated calcifying fluid supplied by seawater (e.g., Gaetani and Cohen, 2006; Gagnon et al., 2012). During this process, elements with a distribution coefficient >1 (such as Ba) are depleted relative to Ca in the isolated calcifying fluid. When the precipitation efficiency is low, the Ba/Ca ratios of the remaining calcifying fluid are high, and the Ba/Ca ratios of the coral skeleton that is precipitated from the remaining fluid are high. We modeled the changes in the Ba/Ca ratios in the coral skeletons based on a closed system Rayleigh fractionation, with the equation following the definitions used by Inoue et al. (2015).

$$Ba/Ca_{coral} = Ba/Ca_{sw} \times (1 - f^{K_D^{Ba/Ca}})/(1 - f)$$

where Ba/Ca_{coral} is the Ba/Ca ratio of the coral skeleton, Ba/Ca_{sw} is the Ba/Ca ratio of the seawater, f (precipitation efficiency, between 0 and 1) is the proportion of Ca remaining in the calcifying fluid after precipitation has ended. The Ba/Ca_{sw} was chosen from the minimum value of 2.43 μmol/mol (the low range of seawater, Shaw et al., 1998) to the maximum value of 8.35 μmol/mol (North Pacific water from a depth of approximately 800 m, ALOHA station, Hsieh and Henderson, 2017). The values of 2.11 and 1.99 were used for $K_D^{Ba/Ca}$ at 25 °C and 29 °C, respectively (Gaetani and Cohen, 2006). The prediction by Rayleigh fractionation seems to be consistent with the observed range of Ba/Ca ratios in our corals (Fig. 4A).

Rayleigh fractionation should also affect Ba isotopes in corals, and the $\delta^{138/134}Ba$ values were calculated using the following equation:

$$\delta^{138/134}Ba_{coral} = (\delta^{138/134}Ba_{sw} + 1000) \times (1 - f^{\alpha})/(1 - f) - 1000$$

where $\delta^{138/134}Ba_{coral}$ is the calculated Ba isotope ratio of the coral skeleton, $\delta^{138/134}Ba_{sw}$ is the Ba isotope ratio of seawater, and α is the isotope fractionation factor. The minimum value of $\delta^{138/134}Ba_{sw}$ was set to 0.34‰, which is the composition of North Pacific water from a depth of approximately 800 m (Hsieh and Henderson, 2017). The maximum value of $\delta^{138/134}Ba_{sw}$ was set to 0.63‰, which is the composition of North Pacific surface water (Hsieh and Henderson, 2017). The fractionation factor (α) between coral and seawater used in this study was 0.9997, which was estimated in Section 4.1 ($\Delta^{138/134}Ba_{coral\text{-}seawater} \sim -0.3‰$). However, the calculated $\delta^{138/134}Ba_{coral}$ values were completely different from the measured $\delta^{138/134}Ba$ values in corals (Fig. 4B). It appears that Rayleigh fractionation does not play a significant role in controlling the Ba isotopic compositions/Ba incorporation of shallow-water corals.

A similar observation in *Porites* corals from New Caledonia was reported by Rollion-Bard et al. (2009). They found that the Li/Ca ratios of corals exhibited a large variation following the Rayleigh fractionation model, but the Li isotopes were homogeneous and could not be explained by the Rayleigh fractionation model. The Li isotope

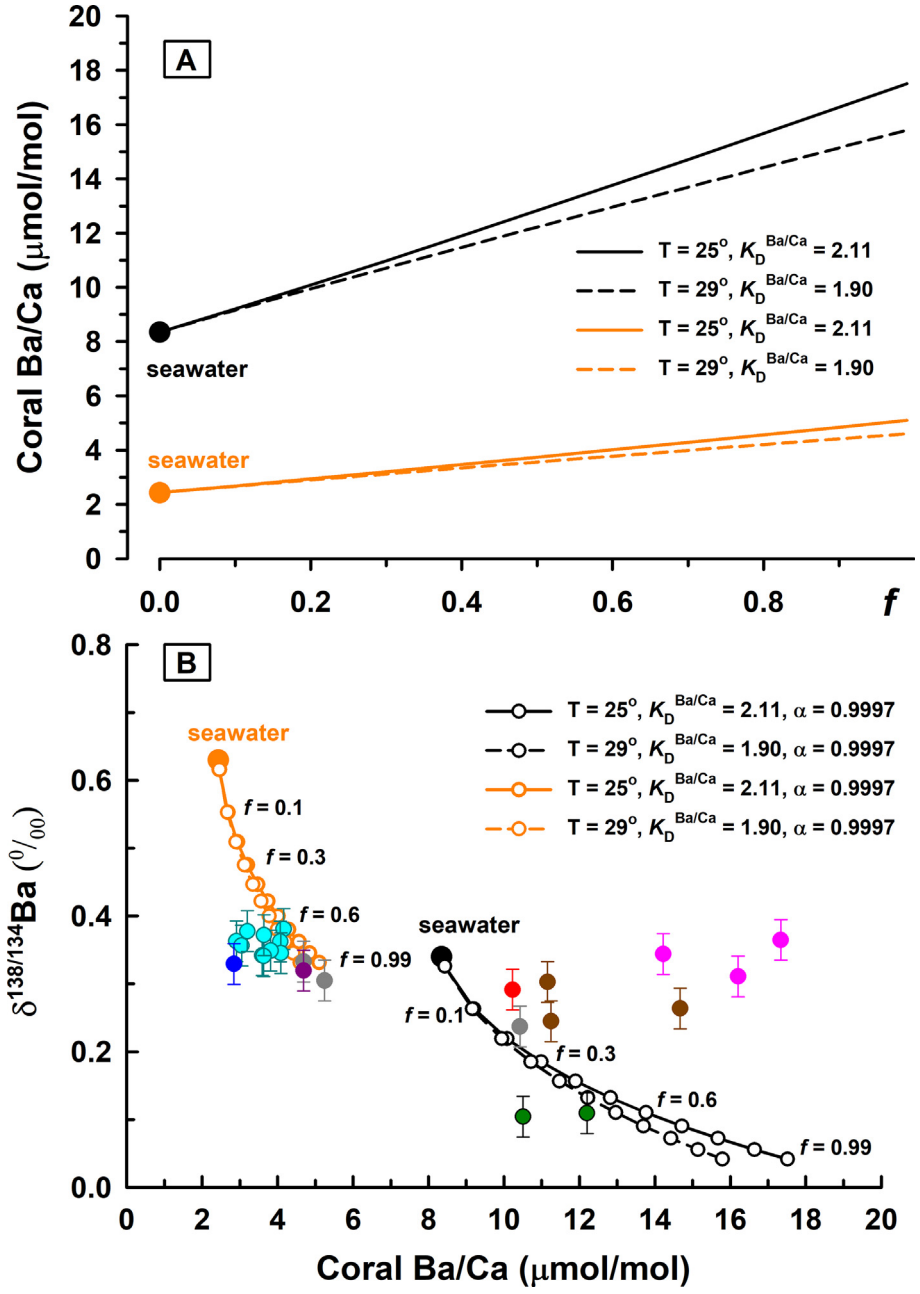

Fig. 4. Modeled Rayleigh-type fractionation of Ba/Ca ratios and Ba isotopes (black and orange lines) during aragonite precipitation. (A) The Ba/Ca ratios of corals vs. *f*—the proportion of Ca remaining in the calcifying fluid. (B) Ba isotope fractionations vs. Ba/Ca ratios in corals with different seawater compositions. See details in the text. (For interpretation of the references to color in this figure legend, the reader is referred to the web version of this article.)

fractionation between seawater and coral aragonite was constant. The authors explained that the disagreement between the Li isotope data and the Rayleigh fractionation model was due to a large reservoir of Li in the calcifying fluid compared to the small amount Li incorporated into the coral skeleton. However, in contrast to Li, Ba is not discriminated in the aragonite lattice, as the distribution coefficient of Ba/Ca is greater than 1. This result implies that if the Ba/Ca ratio in corals is strongly affected by the Rayleigh process, Ba isotopes should also be strongly affected. The behaviors of other alkali earth metals during incorporation in carbonates are in good agreement with the Ba behaviors. Previous research on Sr and Ca in corals supported that the Rayleigh fractionation model is incompatible with Sr and Ca isotopes (in terms of $\delta^{88/86}$Sr and $\delta^{44/40}$Ca) and Sr/Ca ratios in corals (Inoue et al., 2015; Fruchter et al., 2016).

Instead of Rayleigh fractionation, the incorporation of Ba into coral skeletons may be affected by the aragonite saturation state (Ω) of the calcifying fluid. Corals are

known for internal pH and Ω upregulation (McCulloch et al., 2017). In the calcifying fluid of a coral, pH_{cf} is actively elevated by 0.3 to 0.6 pH units above the values in ambient seawater, and Ω_{cf} (10–25) could be several times higher than that in ambient seawater Ω_{sw} (3–4) (McCulloch et al., 2017). In these extremely oversaturated calcifying fluids, small amounts of witherite ($BaCO_3$) could be precipitated within the domains of aragonite, given that witherite is less soluble than aragonite (Mavromatis et al., 2018). This scenario of the formation of two mineral phases was proposed by recent abiotic aragonite experiments, which showed a continuous increase in $K_D^{Ba/Ca}$ as a function of Ω (DeCarlo et al., 2015; Gonneea et al., 2017; Mavromatis et al., 2018). When the Ω of a fluid was greater than 25, the measured $K_D^{Ba/Ca}$was greater than 2 (DeCarlo et al., 2015; Gonneea et al., 2017). However, when Ω was < 2 and the reactive fluid was undersaturated with respect to witherite, the measured $K_D^{Ba/Ca}$ was less than 1 (Mavromatis et al., 2018). Hence, the variations in carbonate chemistry (Ω_{cf} and mineral phases) could potentially explain the large variability in coral Ba/Ca ratios with undisturbed Ba isotopes.

Different results were observed by Pretet et al. (2016). The bulk samples from cultured corals (*Acropora, Montipora*, *Stylophora* and *Porites*) analyzed in their study revealed large Ba isotopic variations ($\delta^{138/134}Ba$ varied between 0.25 ± 0.12‰ and 0.61 ± 0.12‰) (Supplementary Fig. S3). The presence of $\delta^{138/134}$Ba variability in corals grown under identical environmental conditions in an aquarium was interpreted to reflect that Ba isotope fractionation might be governed by the efficiency of Ba incorporation (Rayleigh fractionation) during the biomineralization process (Pretet et al., 2016). However, most of the observed variations are close to the analytical uncertainty (Pretet et al. 2016). In addition, the large variation possibly stemmed from genus dependence. Further research is needed to test whether other coral genera also show the same constant $\delta^{138/134}$Ba fractionation offset as observed for *Porites* in our study from the SCS.

5. CONCLUSIONS

This study is the first to analyze both the skeletal Ba isotopic composition ($\delta^{138/134}$Ba) and the Ba/Ca ratios for shallow-water corals (*Porites*) collected from diverse marine environments throughout the SCS. One of the key observations from our data is that the annual Ba/Ca ratios in corals can vary significantly depending on location by a factor of ~7, whereas $\delta^{138/134}$Ba values exhibit a very limited variation. Our results support the growing body of evidence that Ba incorporation in corals is not a simple function of seawater composition, and coral Ba/Ca ratios must be carefully interpreted to reflect the absolute changes in seawater Ba concentrations. The $\delta^{138/134}$Ba isotope ratios of these shallow-water corals show a relatively constant fractionation offset from surface seawater and are not influenced by environmental parameters such as temperature or rainfall or by different coral growth rates. We suggest that *Porites* corals offer a promising archive to reconstruct the Ba isotopic composition of historical water masses and hence provide new insights into the Ba budget of the ocean and associated oceanic processes on long timescales. For example, riverine Ba inputs to the SCS linked with monsoon intensity through the Holocene could be recorded by the Ba isotopic compositions of coastal corals. Moreover, strong "vital effects" are found for C and O isotopes but not for the Ba isotopes. Thus, Ba isotopes might be used to investigate inorganic environmental factors and decipher biological effects that are expected to cause "vital effects" during mineralization. Further knowledge may be obtained by including additional trace elements and isotopes for an extended multiproxy approach.

ACKNOWLEDGMENTS

This research was supported by the National Science Foundation of China (41630206, 41572148, 41503001), the Open Foundation of the State Key Laboratory of Loess and Quaternary Geology (SKLLQG1613) and a fund from the Youth Innovation Promotion Association, CAS (2017498). This study was also partially supported by the Science Vanguard Research Program of the Ministry of Science and Technology, Taiwan (106-2628-M-002-013, 107-2119-M-002-051 to C.-C.S.), the Higher Education Sprout Project of the Ministry of Education, Taiwan (107L901001 to C.-C.S.). T. F. acknowledges support through DFG-Research Center/Cluster of Excellence "The Ocean in the Earth System" at University of Bremen. We thank Dr. Hong-Wei Chiang for helping to collect corals in Nanwan and Xiaoliuqiu.

APPENDIX A. SUPPLEMENTARY MATERIAL

Supplementary data to this article can be found online at https://doi.org/10.1016/j.gca.2018.12.022.

REFERENCES

Alibert C. and Kinsley L. (2008) A 170-year Sr/Ca and Ba/Ca coral record from the western Pacific warm pool: 1. What can we learn from an unusual coral record? *J. Geophys. Res.* **113**. https://doi.org/10.1029/2006jc003979.

Bates S. L., Hendry K. R., Pryer H. V., Kinsley C. W., Pyle K. M., Woodward E. M. S. and Horner T. J. (2017) Barium isotopes reveal role of ocean circulation on barium cycling in the Atlantic. *Geochim. Cosmochim. Acta* **204**, 286–299. https://doi.org/10.1016/j.gca.2017.01.043.

Becker A., Finger P., Meyer-Christoffer A., Rudolf B. and Ziese M. (2011) *GPCC full data reanalysis version 7.0 at 0.5: Monthly land-surface precipitation from rain-gauges built on GTS-based and historic data*.

Bishop J. K. B. (1988) The barite-opal-organic carbon association in oceanic particulate matter. *Nature* **332**, 341–343. https://doi.org/10.1038/332341a0.

Böttcher M. E., Neubert N., von Allmen K., Samankassou E. and Nägler T. F. (2018) Barium isotope fractionation during the experimental transformation of aragonite to witherite and of gypsum to barite, and the effect of ion (de)solvation. *Isot. Environ. Health Stud.* **54**, 1–12.

Böttcher M. E., Neubert N., Eschera P., von Allmen K., Samankassou E. and Nägler T. F. (in press) isotope Multi-. *Chem. Erde* (in press).

Bridgestock L., Hsieh Y. T., Porcelli D., Homoky W. B., Bryan A. and Henderson G. M. (2018) Controls on the barium isotope compositions of marine sediments. *Earth Planet. Sci. Lett.* **481**, 101–110. https://doi.org/10.1016/j.epsl.2017.10.019.

Bruland K. W. and Lohan M. C. (2003) Controls of trace metals in seawater. In *The oceans and marine geochemistry* (ed. H. Elderfield). Elsevier, London, pp. 23–49.

Bullen T. and Chadwick O. (2016) Ca, Sr and Ba stable isotopes reveal the fate of soil nutrients along a tropical climosequence in Hawaii. *Chem. Geol.* **422**, 25–45. https://doi.org/10.1016/j.chemgeo.2015.12.008.

Cao Z. M., Siebert C., Hathorne E. C., Dai M. H. and Frank M. (2016) Constraining the oceanic barium cycle with stable barium isotopes. *Earth Planet. Sci. Lett.* **434**, 1–9. https://doi.org/10.1016/j.epsl.2015.11.017.

DeCarlo T. M., Gaetani G. A., Holcomb M. and Cohen A. L. (2015) Experimental determination of factors controlling U/Ca of aragonite precipitated from seawater: Implications for interpreting coral skeleton. *Geochim. Cosmochim. Acta* **162**, 151–165.

Dehairs F., Shopova D., Ober S., Veth C. and Goeyens L. (1997) Particulate barium stocks and oxygen consumption in the Southern Ocean mesopelagic water column during spring and early summer: relationship with export production. *Deep Sea Res. Part II* **44**, 497–516. https://doi.org/10.1016/S0967-0645(96)00072-0.

Felis T. and Pätzold J. (2003) Climate records from corals. In *Marine Science Frontiers for Europe* (eds. G. Wefer, F. Lamy and F. Mantoura). Springer-Verlag, Berlin, pp. 11–27.

Fruchter N., Eisenhauer A., Dietzel M., Fietzke J., Bohm F., Montagna P., Stein M., Lazar B., Rodolfo-Metalpa R. and Erez J. (2016) $^{88}Sr/^{86}Sr$ fractionation in inorganic aragonite and in corals. *Geochim. Cosmochim. Acta* **178**, 268–280. https://doi.org/10.1016/j.gca.2016.01.039.

Gaetani G. A. and Cohen A. L. (2006) Element partitioning during precipitation of aragonite from seawater: A framework for understanding paleoproxies. *Geochim. Cosmochim. Acta* **70**, 4617–4634. https://doi.org/10.1016/j.gca.2006.07.008.

Gagnon A. C., Adkins J. F. and Erez J. (2012) Seawater transport during coral biomineralization. *Earth Planet. Sci. Lett.* **329**, 150–161. https://doi.org/10.1016/j.epsl.2012.03.005.

Gonneea M. E., Cohen A. L., DeCarlo T. M. and Charette M. A. (2017) Relationship between water and aragonite barium concentrations in aquaria reared juvenile corals. *Geochim. Cosmochim. Acta* **209**, 123–134. https://doi.org/10.1016/j.gca.2017.04.006.

Hathorne E. C., Gagnon A., Felis T., Adkins J., Asami R., Boer W., Caillon N., Case D., Cobb K. M., Douville E., deMenocal P., Eisenhauer A., Garbe-Schönberg D., Geibert W., Goldstein S., Hughen K., Inoue M., Kawahata H., Kölling M., Le Cornec F. L., Linsley B. K., McGregor H. V., Montagna P., Nurhati I. S., Quinn T. M., Raddatz J., Rebaubier H., Robinson L., Sadekov A., Sherrell R., Sinclair D., Tudhope A. W., Wei G., Wong H., Wu H. C. and You C.-F. (2013) Interlaboratory study for coral Sr/Ca and other element/Ca ratio measurements. *Geochem. Geophys. Geosyst.* **14**, 3730–3750.

Hemsing F., Hsieh Y.-T., Bridgestock L., Spooner P. T., Robinson L. F., Frank N. and Henderson G. M. (2018) Barium isotopes in cold-water corals. *Earth Planet. Sci. Lett.* **491**, 183–192.

Hofmann A. E., Bourg I. C. and DePaolo D. J. (2012) Ion desolvation as a mechanism for kinetic isotope fractionation in aqueous systems. *Proc. Natl. Acad. Sci. USA* **109**, 18689–18694. https://doi.org/10.1073/pnas.1208184109.

Horner T. J., Kinsley C. W. and Nielsen S. G. (2015) Barium-isotopic fractionation in seawater mediated by barite cycling and oceanic circulation. *Earth Planet. Sci. Lett.* **430**, 511–522. https://doi.org/10.1016/j.epsl.2015.07.027.

Hsieh Y. T. and Henderson G. M. (2017) Barium stable isotopes in the global ocean: Tracer of Ba inputs and utilization. *Earth Planet. Sci. Lett.* **473**, 269–278. https://doi.org/10.1016/j.epsl.2017.06.024.

Inoue M., Gussone N., Koga Y., Iwase A., Suzuki A., Sakai K. and Kawahata H. (2015) Controlling factors of Ca isotope fractionation in scleractinian corals evaluated by temperature, pH and light controlled culture experiments. *Geochim. Cosmochim. Acta* **167**, 80–92. https://doi.org/10.1016/j.gca.2015.06.009.

Jacquet S. H. M., Dehairs F., Cardinal D., Navez J. and Delille B. (2005) Barium distribution across the Southern Ocean frontal system in the Crozet-Kerguelen Basin. *Mar. Chem.* **95**, 149–162. https://doi.org/10.1016/j.marchem.2004.09.002.

LaVigne M., Grottoli A. G., Palardy J. E. and Sherrell R. M. (2016) Multi-colony calibrations of coral Ba/Ca with a contemporaneous in situ seawater barium record. *Geochim. Cosmochim. Acta* **179**, 203–216. https://doi.org/10.1016/j.gca.2015.12.038.

Lea D. W., Shen G. T. and Boyle E. A. (1989) Coralline barium records temporal variability in equatorial pacific upwelling. *Nature* **340**, 373–376. https://doi.org/10.1038/340373a0.

Mavromatis V., van Zuilen K., Purgstaller B., Baldermann A., Nagler T. F. and Dietzel M. (2016) Barium isotope fractionation during witherite ($BaCO_3$) dissolution, precipitation and at equilibrium. *Geochim. Cosmochim. Acta* **190**, 72–84. https://doi.org/10.1016/j.gca.2016.06.024.

Mavromatis V., Goetschl K. E., Grengg C., Konrad F., Purgstaller B. and Dietzel M. (2018) Barium partitioning in calcite and aragonite as a function of growth rate. *Geochim. Cosmochim. Acta* **237**, 65–78. https://doi.org/10.1016/j.gca.2018.06.018.

McCulloch M., Fallon S., Wyndham T., Hendy E., Lough J. and Barnes D. (2003) Coral record of increased sediment flux to the inner Great Barrier Reef since European settlement. *Nature* **421**, 727–730. https://doi.org/10.1038/nature01361.

McCulloch M., D'Olivo J. P., Falter J., Holcomb M. and Trotter J. (2017) Coral calcification in a changing world and the interactive dynamics of pH and DIC up-regulation. *Nat. Comm.* **8**, 15686. https://doi.org/10.1038/ncomms15686.

Miyazaki T., Kimura J. I. and Chang Q. (2014) Analysis of stable isotope ratios of Ba by double-spike standard-sample bracketing using multiple-collector inductively coupled plasma mass spectrometry. *J. Anal. At. Spectrom.* **29**, 483–490. https://doi.org/10.1039/c3ja50311a.

Montaggioni L. F., Le Cornec F., Correge T. and Cabioch G. (2006) Coral barium/calcium record of mid-Holocene upwelling activity in New Caledonia, South-West Pacific. *Palaeogeogr. Palaeoclimatol. Palaeoecol.* **237**, 436–455. https://doi.org/10.1016/j.palaeo.2005.12.018.

Moyer R. P., Grottoli A. G. and Olesik J. W. (2012) A multiproxy record of terrestrial inputs to the coastal ocean using minor and trace elements (Ba/Ca, Mn/Ca, Y/Ca) and carbon isotopes ($\delta^{13}C$, $\Delta^{14}C$) in a nearshore coral from Puerto Rico. *Paleoceanography* **27**. https://doi.org/10.1029/2011pa002249.

Nan X. Y., Wu F., Zhang Z. F., Hou Z. H., Huang F. and Yu H. M. (2015) High-precision barium isotope measurements by MC-ICP-MS. *J. Anal. At. Spectrom.* **30**, 2307–2315. https://doi.org/10.1039/c5ja00166h.

Okai T., Suzuki A., Kawahata H., Terashima S. and Imai N. (2002) Preparation of a new Geological Survey of Japan geochemical reference material: Coral JCp-1. *Geostand. Newsletter J. Geostand. Geoanal.* **26**, 95–99. https://doi.org/10.1111/j.1751-908X.2002.tb00627.x.

Paytan A. and Griffith E. M. (2007) Marine barite: Recorder of variations in ocean export productivity. *Deep Sea Res. Part II* **54**, 687–705. https://doi.org/10.1016/j.dsr2.2007.01.007.

Paytan A. and Kastner M. (1996) Benthic Ba fluxes in the central Equatorial Pacific, implications for the oceanic Ba cycle. *Earth Planet. Sci. Lett.* **142**, 439–450. https://doi.org/10.1016/0012-821x(96)00120-3.

Pretet C., Van Zuilen K., Nagler T. F., Reynaud S., Bottcher M. E. and Samankassou E. (2016) Constraints on barium isotope fractionation during aragonite precipitation by corals. *Depositional Rec.* **1**, 118–129. https://doi.org/10.1002/dep2.8.

Raddatz J., Liebetrau V., Ruggeberg A., Hathorne E., Krabbenhoft A., Eisenhauer A., Bohm F., Vollstaedt H., Fietzke J., Lopez Correa M., Freiwald A. and Dullo W. C. (2013) Stable Sr-isotope, Sr/Ca, Mg/Ca, Li/Ca and Mg/Li ratios in the scleractinian cold-water coral Lophelia Pertusa. *Chem. Geol.* **352**, 143–152. https://doi.org/10.1016/j.chemgeo.2013.06.013.

Reynolds R. W., Rayner N. A., Smith T. M., Stokes D. C. and Wang W. Q. (2002) An improved in situ and satellite SST analysis for climate. *J. Clim.* **15**, 1609–1625. https://doi.org/10.1175/1520-0442(2002) 015<1609:Aiisas>2.0.Co;2.

Rollion-Bard C., Vigier N., Meibom A., Blamart D., Reynaud S., Rodolfo-Metalpa R., Martin S. and Gattuso J. P. (2009) Effect of environmental conditions and skeletal ultrastructure on the Li isotopic composition of scleractinian corals. *Earth Planet. Sci. Lett.* **286**, 63–70. https://doi.org/10.1016/j.epsl.2009.06.015.

Rollion-Bard C., Blamart D., Cuif J. P. and Dauphin Y. (2010) In situ measurements of oxygen isotopic composition in deep-sea coral, Lophelia pertusa: re-examination of the current geochemical models of biomineralization. *Geochim. Cosmochim. Acta* **74**, 1338–1349. https://doi.org/10.1016/j.gca.2009.11.011.

Saha N., Webb G. E. and Zhao J. X. (2016) Coral skeletal geochemistry as a monitor of inshore water quality. *Sci. Total Environ.* **566**, 652–684. https://doi.org/10.1016/j.scitotenv.2016.05.066.

Schlitzer R. (2018) *Ocean Data View*.

Shaw T. J., Moore W. S., Kloepfer J. and Sochaski M. A. (1998) The flux of barium to the coastal waters of the southeastern USA: The importance of submarine groundwater discharge. *Geochim. Cosmochim. Acta* **62**, 3047–3054. https://doi.org/10.1016/S0016-7037(98)00218-X.

Sinclair D. J. (2005) Non-river flood barium signals in the skeletons of corals from coastal Queensland, Australia. *Earth Planet. Sci. Lett.* **237**, 354–369. https://doi.org/10.1016/j.epsl.2005.06.039.

Tudhope A. W., Lea D. W., Shimmield G. B., Chilcott C. P. and Head S. (1996) Monsoon climate and Arabian sea coastal upwelling recorded in massive corals from southern Oman. *Palaios* **11**, 347–361. https://doi.org/10.2307/3515245.

von Allmen K., Bottcher M. E., Samankassou E. and Nagler T. F. (2010) Barium isotope fractionation in the global barium cycle: First evidence from barium minerals and precipitation experiments. *Chem. Geol.* **277**, 70–77. https://doi.org/10.1016/j.chemgeo.2010.07.011.

Weldeab S., Lea D. W., Schneider R. R. and Andersen N. (2007) 155,000 years of West African monsoon and ocean thermal evolution. *Science* **316**, 1303–1307. https://doi.org/10.1126/science.1140461.

Wombacher F., Eisenhauer A., Böhm F., Gussone N., Regenberg M., Dullo W.-C. and Rüggeberg A. (2011) Magnesium stable isotope fractionation in marine biogenic calcite and aragonite. *Geochim. Cosmochim. Acta* **75**, 5797–5818.

Zeng Z., Li X., Liu Y., Huang F. and Yu H. M. (in press) High-precision barium isotope measurements of carbonates by MC-ICP-MS. *Geostand. Geoanal. Res.* (in press).

Associate editor: Claudine Stirling